# Atomic structure of alloy surfaces. II. Ni₃Al{111}

ΩTIC FILE COPY

D. Sondericker* and F. Jona

*College of Engineering and Applied Science, State University of New York at Stony Brook, Stony Brook, New York 11794-2275*

P. M. Marcus

*IBM Thomas J. Watson Research Center, P.O. Box 218, Yorktown Heights, New York 10598*

A low-energy-electron-diffraction intensity analysis of a clean Ni₃Al{111} surface reveals a structure that is essentially bulklike, but with a slight buckling of the first atomic layer. The plane of the Al atoms is moved outwards to a position 0.06±0.03 Å from the plane of the Ni atoms, which is in turn very slightly shifted inward (0.01±0.03 Å) toward the second atomic layer. Second and deeper interlayer spacings are expected to be equal to the bulk value (2.055 Å). The *r*-factor values for both normal (0.13) and oblique (0.16) incidence correspond to a very good fit of theory to experiment.

## I. INTRODUCTION

There is increasing interest, of late, in the atomic structure of surfaces of metallic alloys, in part because very little is known about this subject and in part because one wishes to establish to what extent the phenomenon of multilayer relaxation, discovered by low-energy electron diffraction (LEED) on the surfaces of pure metals,[1] occurs on surfaces of metallic alloys. In addition, alloys and compounds have an extra degree of freedom in that the surface layers can buckle, i.e., a different relaxation of the sublattices can occur. In general, studies of alloys are more difficult than those of pure metals for several reasons, among them: (1) single crystals of alloys are not easily available in convenient sizes (at least a few millimeters across), (2) of those crystals that are available only a limited number have small, and hence easily treatable, unit cells, (3) alloys have relatively more phases as a function of temperature than pure metals, and (4) the presence of more than one atom in the unit cell complicates the structure determination; in the case of LEED, this fact lengthens the required computer calculations, often considerably. To date, only the structures of three alloy surfaces have been studied by quantitative LEED intensity analysis and reported in the literature [Ni₃Al{001},[2] NiAl{110}[3], and α-CuAl{111} with bulk Al concentration of 16 at. % (Refs. 4 and 5)], but others are in progress, both by quantitative LEED [Ni₃Al{110} (Ref. 6), Cu₃Au {001} and {111} (Ref. 6), Pt₃Ti{001} (Ref. 7), and Pt_xNi_{1-x}{111} (Ref. 8)], qualitative LEED [Ni₃Ir {001}, {111}, and {110} (Ref. 9)], and medium-energy ion scattering [NiAl{110} (Ref. 10)].

The present report concerns the atomic structure of a {111} surface of Ni₃Al, an ordered alloy with the bulk structure of Cu₃Au (Fig. 1). The structure of a {001} surface of Ni₃Al was studied by LEED intensity analysis and reported by us in the literature recently.[2] We will refer to that report as paper I. There are two possible {001} terminations but the analysis described in paper I shows that only one occurs in practice, with 50% Ni–50% Al composition in the first and 100% Ni in the second layer. No

such choice exists for the {111} termination because all {111} planes (one of which is indicated with thick lines in Fig. 1) are equal to one another, with the stoichiometric composition of three Ni and one Al atoms. The structure was determined by means of a LEED intensity analysis assisted by Auger-electron spectroscopy (AES) as described below. We discuss the experiment in Sec. II, the analysis and the results in Sec. III, and the conclusion in Sec. IV.

## II. EXPERIMENT

The {111} sample used in the present study came from the same ingot that provided the {001} sample analyzed in paper I. A larger grain was identified in the ingot by
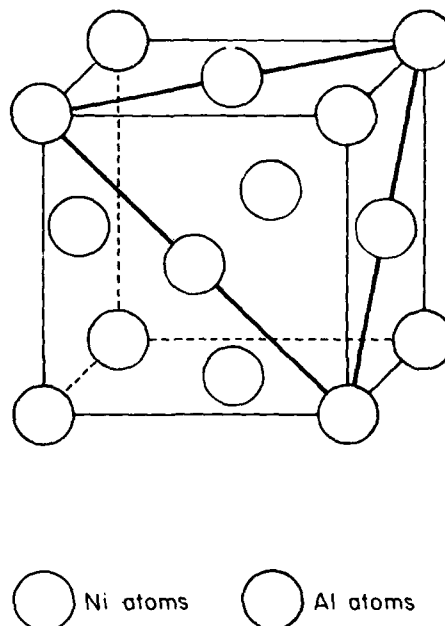


FIG. 1. Schematic view of the unit cell of Ni₃Al. A {111} plane is outlined with thick lines.

○ Ni atoms          ○ Al atoms

etching the surface with dilute $HNO_3$. Because of its small dimensions (final size $2\times2$ mm$^2$) and for ease of handling, the grain was left imbedded in the ingot's polycrystalline matrix and was oriented within a few degrees of {111} by means of Laue diffraction patterns. It was then spark-erosion cut to expose the largest possible {111} surface and carefully reoriented and sanded with fine emery paper to achieve the {111} orientation within $\pm0.5°$. The surface was then lapped with a sequence of finer and finer alumina pastes and finally polished with 0.03-$\mu$m alumina slurry.[11] No further treatment of the surface was applied prior to introduction into the vacuum system other than standard washing and degreasing. The sample was wrapped in 0.05-mm-thick Ta foil with the {111} surface exposed. In the vacuum system, heating of the sample was accomplished by electron bombardment of the Ta foil to the back of the sample. After attainment of base pressure ($<1\times10^{-10}$ torr) the {111} surface was cleaned with a series of cycles of Ar-ion sputtering treatments at room temperature for one hour followed by one-hour anneals at 800–850°C. Twenty-five cycles were needed to reduce surface impurities (sulfur, carbon, and oxygen) to trace levels, as detected by AES.

Surface composition was also monitored by AES during and after the annealing treatments. In Fig. 2 we plot the ratio $R_A$ $[=I(Al_{68eV})/I(Ni_{61eV})]$ between the intensity of the Al AES line at 68 eV and the intensity of the Ni AES line at 61 eV. These intensities were measured as discussed in paper I (footnote 2). We see in Fig. 2 that immediately after Ar bombardment $R_A$ was about 0.6, just as on the {001} surface. After 10-min anneals at the temperatures indicated in the figure, $R_A$ increased monotonically and reached a plateau at about 700°C. For temperatures higher than 750°C, the value of $R_A$ increased again but slow cooling of the sample caused $R_A$ to decrease, receding approximately to the plateau value (0.7) at room temperature. This behavior is similar to that observed on

the {001} surface and has the same explanation. Since aluminum is preferentially sputtered, the surface composition after one hour of Ar bombardment is about the same on {111} as on {001}. Upon heating, Al diffuses to the surface until it reaches an equilibrium concentration (which now, after determination of the surface structure, we know to be bulklike). We note that the equilibrium value of $R_A$ on {111} (0.7) is smaller than that achieved on {001} (0.95), an indication that the concentration of Al is less on {111} than on {001}, as confirmed quantitatively by the LEED analysis. Temperatures higher than 750°C cause further segregation of Al on the surface but this condition is not stable at lower temperatures and upon cooling the excess Al diffuses back into the bulk until the equilibrium (bulklike) composition is achieved. This surface composition is stable between room temperature and 750°C. It is this surface that was subjected to the LEED study.

The LEED pattern was sharp and with low background. Intensity data were collected with the computer-
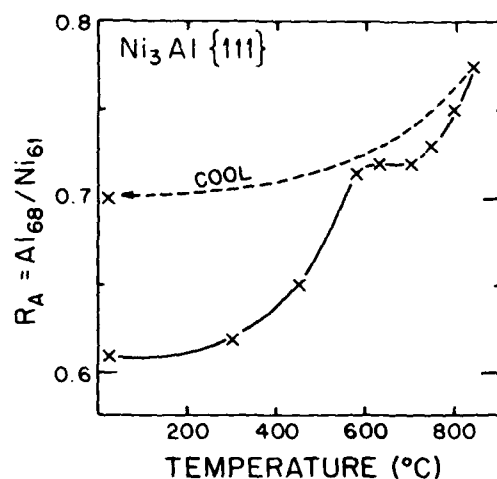


FIG. 2. Dependence of the ratio $R_A$ between the AES line of Al at 68 eV and the AES line of Ni at 61 eV upon thermal treat- ... of Ni₃Al{111} surface after Ar-ion bombardment. The crosses represent 10-min anneals at the corresponding temperatures.

TABLE I. Beam indices, $r$ (reliability) factors, and energy ranges for Ni₃Al{111} at normal incidence. $V_0=12$ eV.

| Beam | r factor | ΔE |
|---|---|---|
| 10 | 0.0802 | 169 |
| 1̄1 | 0.1487 | 169 |
| 01̄ | 0.0811 | 169 |
| 1̄0 | 0.0510 | 169 |
| 11̄ | 0.0638 | 169 |
| 2̄0 | 0.0923 | 132 |
| 22̄ | 0.0931 | 132 |
| 20 | 0.1219 | 134 |
| 2̄2 | 0.1010 | 133 |
| 02̄ | 0.1286 | 138 |
| 2̄1 | 0.0634 | 152 |
| 21̄ | 0.0690 | 149 |
| 1̄1̄ | 0.1415 | 152 |
| 12̄ | 0.1214 | 152 |
| 3̄1 | 0.2092 | 66 |
| 3̄2 | 0.2291 | 66 |
| 2̄1̄ | 0.1854 | 102 |
| 23̄ | 0.1983 | 102 |
| 3̄2 | 0.1449 | 102 |
| 1̄2̄ | 0.1541 | 102 |
| 31̄ | 0.2800 | 90 |
| 13̄ | 0.1986 | 102 |
| 2̄2̄ | 0.2569 | 62 |
| 24̄ | 0.2264 | 62 |
| 3̄0 | 0.1881 | 57 |
| 33̄ | 0.1388 | 57 |
| 30 | 0.1855 | 52 |
| 3̄3 | 0.1352 | 57 |
| 03̄ | 0.0694 | 57 |
| Mean | 0.1283 | 3255 |

TABLE II. Beam indices, $r$ (reliability) factors and energy ranges for $Ni_3Al\{111\}$ at $\theta=15°$, $\phi=-60°$. $V_0=12$ eV.

| Beam | $r$ factor | $\Delta E$ |
|------|-----------|-----------|
| 00 | 0.0955 | 169 |
| 10 | 0.1649 | 92 |
| 0Ī | 0.2093 | 92 |
| Ī0 | 0.1215 | 169 |
| 01 | 0.1027 | 169 |
| Ī1 | 0.1470 | 169 |
| 11 | 0.1020 | 81 |
| ĪĪ | 0.0823 | 82 |
| 02 | 0.2209 | 142 |
| 2̄0 | 0.1560 | 144 |
| Ī2 | 0.1125 | 128 |
| 2̄1 | 0.0888 | 169 |
| 2̄2 | 0.1663 | 52 |
| 3̄0 | 0.3181 | 82 |
| 03 | 0.3831 | 72 |
| 3̄1 | 0.0537 | 131 |
| 4̄1 | 0.5674 | 87 |
| 4̄2 | 0.2124 | 122 |
| 5̄3 | 0.1477 | 72 |
| Mean | 0.1649 | 2225 |



FIG. 3. Examples of very good agreement between theory and experiment. The numbers over each experimental curve are $r$-factor values.

controlled television-camera system described elsewhere.[12] The analysis was done with 29 degenerate (10 nondegenerate) spectra at normal incidence, and 19 degenerate (13 nondegenerate) spectra at $\theta=15°$, $\phi=-60°$. For the definitions of $\theta$ and $\phi$, see, e.g., Ref. 13. The data were normalized to constant incident current, the energy values were corrected for the contact-potential difference (3.2 eV) between sample and cathode of the electron gun, and the intensities were corrected for background.

## III. ANALYSIS

The calculations of LEED intensities were done with the CHANGE program described elsewhere[14] and with values of the nonstructural parameters similar to those discussed in paper I [ $V_0=-(12+3.5i)$ eV, 6 phase shifts, 55 beams]. The first calculations, done for a bulklike model of the surface structure (see the thick outline in Fig. 1), produced substantial agreement with the normal-incidence experimental data, so that only one further model was tested: a model involving a Ni overlayer which, however, worsened the fit to experiment considerably. The refinement of the bulk-like model was started by varying the first interlayer spacing $d_{12}$ by $\pm0.1$ Å about the bulk value (2.055 Å), the three Ni and one Al atoms in the first layer remaining coplanar. The fit to experiment (normal incidence) was evaluated both visually and with
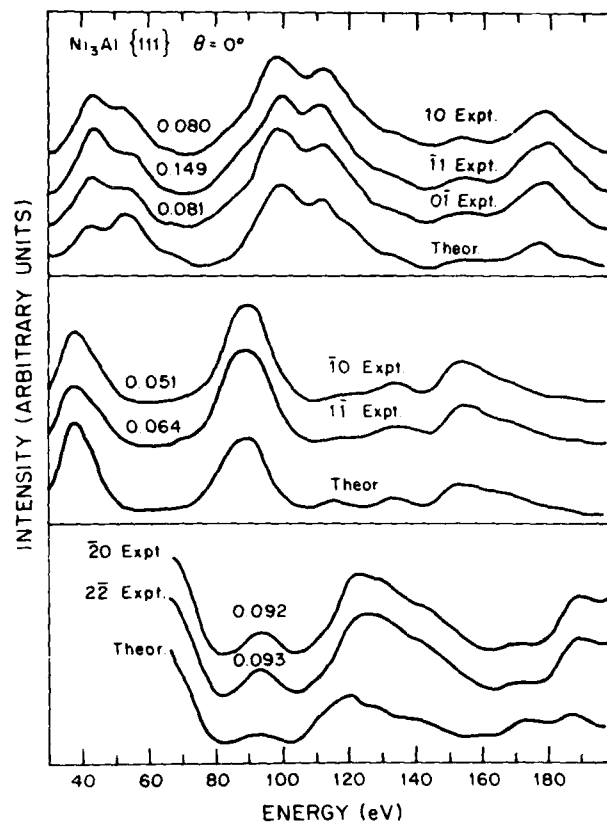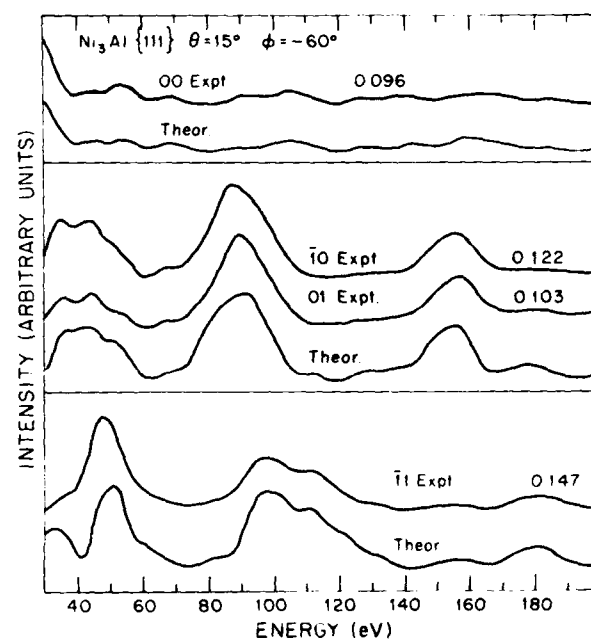


FIG. 4. Examples of good to mediocre agreement between theory and experiment. The numbers over each experimental curve are $r$-factor values.
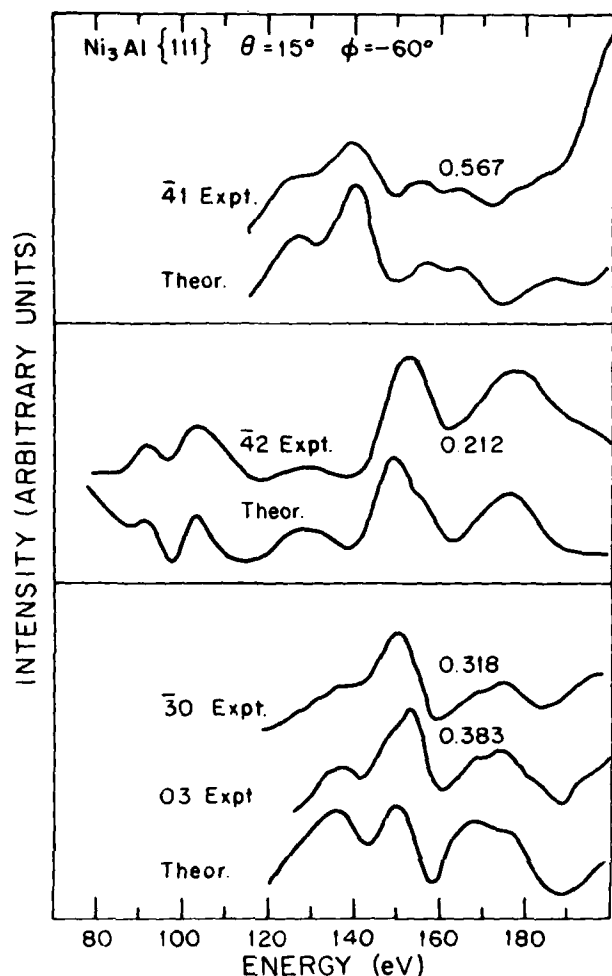
FIG. 5. Examples of bad agreement between theory and experiment. The numbers over each experimental curve are *r*-factor values.



FIG. 6. Schematic side view of the Ni₃Al{111} structure. The Al atoms are 0.06 Å above the Ni atoms in the first layer.

the *r* factor defined elsewhere,[15] which exhibited a minimum for a very slight expansion (0.01±0.03 Å) of $d_{12}$. Because of this almost negligible first-layer relaxation, and because study of deeper relaxations would have involved at least doubling the number of atoms in the surface layer and hence increased the computer time considerably, all interlayer spacings beyond the first were assumed to be equal to the bulk value. However, buckling of the first layer (i.e., out-of-plane motions of the Ni and Al atoms) was tested. Different species in the first layer were allowed to move up or down by 0.1 Å in steps of 0.05 Å, while at the same time the distance between the (rigidly held) buckled first layer and the (planar) second layer was varied. The *r* factor exhibited a minimum for a buckling involving the Al atoms (one per unit mesh) 0.05 Å above the bulk value of $d_{12}$ and the Ni atoms (three per unit mesh) 0.01 Å below the bulk $d_{12}$. Thus, we find a small but detectable buckling of the first atomic layer with the Al atoms 0.06 Å above the Ni atoms.

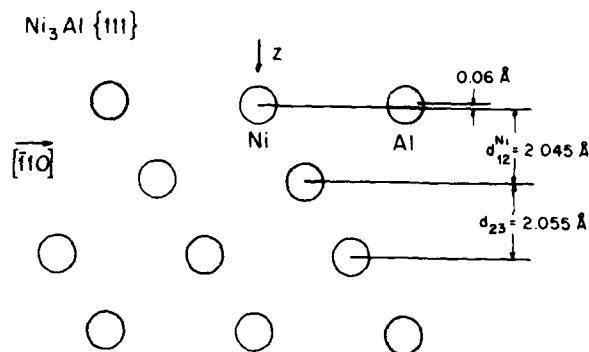The analysis was then extended to the non-normal-incidence data. Calculations were made for the buckled model described above for $\theta = 15°$, $\phi = -60°$, and the minimum in *r* factor was confirmed for the same parameter values determined by the normal-incidence analysis. To test the possibility of (small) errors in the angle of incidence, calculations were also made for $\theta = 13°$ and 17° but the experimental value of $\theta = 15°$ was confirmed as that providing the lowest value of the *r* factor.

Tables I and II present the final results for the data at normal incidence and at $\theta = 15°$, $\phi = -60°$, respectively. The tables list the beam indices and the corresponding values of the *r* factor and the energy interval $\Delta E$ covered by the corresponding LEED spectrum. We see that the mean *r* factor is 0.128 over a total $\Delta E = 3255$ eV for the set at $\theta = 0°$, and 0.165 over a total $\Delta E = 2225$ eV for the set at $\theta = 15°$, $\phi = -60°$. To economize on space and yet give examples of the quality of the fit to experiment we show selected experimental and theoretical spectra in three figures. Examples of very good fit are depicted in Fig. 3, of good and mediocre fit in Fig. 4, and of bad fit in Fig. 5. Overall, both the mean *r*-factor values and the visual evaluation concur in establishing that the agreement between theory (for the model described) and experiment is very good.

## IV. CONCLUSIONS

Figure 6 shows schematically a side view of the Ni₃Al{111} structure. Second and deeper interlayer spacings have the bulk value (2.055 Å). In the first layer the Ni atoms (three per unit mesh) are somewhat closer to the second layer (2.045 Å) than in bulk while the Al atoms (one per unit mesh) are moved out 0.06±0.03 Å with respect to the Ni subplane. Thus, the termination is essentially bulklike but with a small buckling of the top atomic layer.

## ACKNOWLEDGMENTS

*Present address: National Synchrotron Light Source (NSLS), Brookhaven National Laboratory, Upton, NY 11973-5000.

[1]See, e.g., D. L. Adams and C. S. Sorensen, Surf. Sci. 166, 495 (1986).

[2]D. Sondericker, F. Jona, V. L. Moruzzi, and P. M. Marcus, Solid State Commun. 53, 175 (1985); paper I, Phys. Rev. B 33, 900 (1986).

[3]H. L. Davis and J. R. Noonan, Phys. Rev. Lett. 54, 566 (1985).

[4]R. J. Baird, D. F. Ogeltree, M. A. Van Hove, and G. A. Somorjai, Surf. Sci. 165, 345 (1986).

[5]G. L. Berning and W. J. Coleman, Proceedings on the 9th International Vacuum Congress and 5th International Conference on Surface Science, Madrid, 1983, p. 36 (unpublished).

[6]D. Sondericker, F. Jona, and P. M. Marcus, Bull. Am. Phys. Soc. 31, 325 (1986); and to be published.

[7]U. Bardi, M. Torrini, E. Zanazzi, G. Rovida, M. Maglietta, P. N. Ross, and M. A. Van Hove, International Conference on Solid Surfaces-1, Berkeley, California, August 1984 (unpublished).

[8]Y. Gauthier, R. Beaudoing, Y. Joly, J. Rundgren, J. C. Bertolini, and J. Mollardier, Europhysics Conference Abstracts, Vol. 9C (ECOSS-7), p. 284 (unpublished); Surf. Sci. 162, 342 (1985).

[9]S. Sinharoy, A. I. Braginski, J. T. Talvocchio, and E. Walker, Surf. Sci. 167, 401 (1986).

[10]S. M. Yalisove and W. R. Graham, Bull. Am. Phys. Soc. 31, 325 (1986).

[11]The existence of polycrystalline regions around the surface to be studied presented no difficulty for LEED because only the crystal would provide a diffraction pattern. For AES, care was exercised to insure that the primary electron beam would probe only the {111} surface and not the surrounding areas.

[12]F. Jona, J. A. Strozier, Jr., and P. M. Marcus, in The Structure of Surfaces, edited by M. A. Van Hove and S. Y. Tong (Springer, Berlin, 1985), p. 92.

[13]F. Jona, J. Phys. C 11, 4271 (1978).

[14]D. W. Jepsen, H. D. Shih, F. Jona, and P. M. Marcus, Phys. Rev. B 22, 814 (1980).

[15]E. Zanazzi and F. Jona, Surf. Sci. 62, 61 (1977).